

On the Performance of Combined Quadrature Amplitude Modulation and Convolutional Codes for Cross-Coupled Multidimensional Channels

MOHSEN KAVEHRAD, SENIOR MEMBER, IEEE, PETER J. McLANE, SENIOR MEMBER, IEEE, AND
CARL-ERIK W. SUNDBERG, SENIOR MEMBER, IEEE

Abstract—The performance of cross-coupled, M -ary quadrature amplitude modulation (QAM) systems is determined when bandwidth efficient trellis codes are used to combat interference. Performance with and without compensation for cross-coupled interference is presented. It is found that simple trellis codes can maintain the error probability at an acceptable level for cross-coupling parameters that render uncoded systems unusable. Up to two-dimensional trellis codes are considered for four-dimensional QAM signals, and possibilities of obtaining diversity advantages in the form of higher total system throughput by prolonged availability of the two signals are explored. This is accomplished through joint coding over two different constellations. The probability of the most likely error events is calculated by using the method of moments. The results are applicable to any digital communication system using multidimensional quadrature amplitude modulation, e.g., voiceband modems, cross-polarized radio systems and, to some extent, optical systems. In the paper the analysis is restricted to nondispersive cross-coupling models. In most cases the coding gain is larger than in the absence of cross-coupling interference. Specifically, it is found that simple codes have coding gains increased by at least 2 dB with cross-coupling interference relative to that obtained on the additive white Gaussian noise channel.

I. INTRODUCTION

MULTIDIMENSIONAL modulation is becoming a popular technique for digital communication systems requiring high capacity. Examples exist in voiceband modems [1] and in microwave radio systems where two polarizations are used to send independent, quadrature amplitude modulated (QAM) data signals [2]. In such systems the component signals for multidimensional modulation cannot be regarded as being uncoupled. In this paper it is shown that channel coding combined with QAM (trellis coding), with or without compensation for cross-coupling type interference, is an effective means to reduce system performance degradation.

The channel codes considered in the paper are basically the same as the bandwidth efficient trellis codes presented by Ungerboeck [3], who considered their performance for an additive, white Gaussian noise (AWGN) channel. Later Tharpar [4] presented results on the performance of trellis codes for a number of signal impairments that occur in voiceband data transmission. Wei [5] has constructed trellis codes that are suitable for practical systems with differential

encoding/decoding. Trellis codes have been considered for multidimensional modulation by Calderbank and Sloane [6] and Wilson and Sleeper [7], among others. However, their performance studies were for an AWGN channel.

The objective of this paper is to determine the performance of trellis codes for multidimensional QAM signals in the presence of AWGN and cross-coupling between signal dimensions. Performance of coded systems is found with and without a structure that compensates for signal cross-coupling. The cross-coupling is taken to be circularly symmetric and with deterministic coupling coefficients. In some cases the trellis codes utilized are designed to exploit the independence between dimensional cross-coupling as a form of diversity and, hence, realize a total system throughput gain through the prolonged availability of the signals. However, such diversity through coding turns out to be effective only for systems without signal cross-coupling compensation (for the compensator considered here). In any case, trellis codes are always found to exhibit excellent performance in interference channels compared to an additive white Gaussian noise environment.

The method of moments [8] is used to numerically determine, with high precision, the performance of trellis coded systems with cross-coupling interference. The performance of the coded systems is evaluated by calculating the error event probability for the most likely error events. The error event probability can be determined without having to be concerned about the accuracy of upper or lower bounds for the average error event probability. Finally, based on worst case interference considerations, the asymptotic performance for a high value of signal-to-noise ratio (SNR) has also been calculated for the above systems and the results are in good agreement with those obtained by using the method of moments. The asymptotic formulas are very simple, are easy to use, and are quite convenient for approximate coding gain calculations at intermediate SNR values found in practice.

Following the Introduction, in Section II we describe the system model. System performance for the uncoded case, with and without the interference compensator, is presented in Section III. In Section IV performance analysis for the coded systems is presented, and a performance comparison is made with and without the interference compensator. Numerical results are discussed in Section V. Finally, our conclusions are presented in Section VI. Formulas for the moments used in the paper are presented in the Appendix.

II. SYSTEM MODEL

The signal transmission model involves two orthogonal M -ary QAM signals with the same bandwidth and center frequency. Such a signal set can be represented as

$$S_i(t) = \text{Re} \{ \tilde{S}_i(t) \exp(j\omega_c t) \}, \quad i = 1, 2 \quad (1)$$

Paper approved by the Editor for Coding Theory and Applications of the IEEE Communications Society. Manuscript received October 4, 1985; revised March 16, 1986. This paper was presented at the International Conference on Communications, Toronto, Ont., Canada, June 1986.

M. Kavehrad and C.-E. W. Sundberg are with AT&T Bell Laboratories, Holmdel, NJ 07733.

P. J. McLane is with the Department of Electrical Engineering, Queen's University, Kingston, Ont., Canada K7L 3N6.

IEEE Log Number 8611267.

where $\text{Re}\{\cdot\}$ denotes the real part of a complex number, $j = \sqrt{-1}$, $\tilde{S}_i(t)$ is the complex envelope of $S_i(t)$, and ω_c is the carrier frequency in radians per second. The signal $\tilde{S}_i(t)$ is

$$\tilde{S}_i(t) = \sum_{k=0}^{\infty} \tilde{\alpha}_{ik} \tilde{h}(t - kT) \quad i=1, 2 \quad (2)$$

where $\tilde{\alpha}_{ik}$ is the complex data symbol and $\tilde{h}(t)$ is the complex, low-pass equivalent impulse response of the system. The components of $\tilde{S}_i(t)$ modulate the in-phase and quadrature carrier components (rails) of two cross-polarized QAM modulators. The components of $S_i(t)$ are denoted by $(S_{1R}, S_{1I}, S_{2R}, S_{2I})$ since they represent the real and imaginary parts of the complex envelope. Finally, for any k , $\alpha_{ik} = \delta_{ik} + j\beta_{ik}$ where δ_{ik} and β_{ik} are from the set $\{\pm C, \pm 3C, \dots, \pm(L-1)C\}$ with $M = L^2$, the number of signal points in the QAM signal constellation, and C is a constant (one) throughout the paper.

The received signal is $r(t) = A\tilde{S}(t) + n(t)$ where A is a 2×2 complex matrix which models the cross-coupling between the signals $\tilde{S}_i(t)$, $i = 1, 2$ and $\tilde{S}(t)$ is the complex, two-vector $(\tilde{S}_1(t), \tilde{S}_2(t))$. Also, $n(t)$ is a complex, Gaussian noise vector.

We shall only consider the effect of the noise $n(t)$ and the matrix A on the system error probability. As such it is convenient to write $r(t)$ in vector-matrix form as

$$R = DH + N \quad (3)$$

where for a fixed time-sample

$$R = [r_{1R}, r_{1I}, r_{2R}, r_{2I}] \quad (4)$$

$$D = [\delta_{1k}, \beta_{1k}, \delta_{2k}, \beta_{2k}] \quad (5)$$

$$N = [n_{1R}, n_{1I}, n_{2R}, n_{2I}] \quad (6)$$

In (3)–(6), $r_{iR} = \text{Re}\{r_i(t^*)\}$ and $r_{iI} = \text{Im}\{r_i(t^*)\}$ with $i = 1, 2$, t^* the sample time for detection, and $\text{Im}\{\cdot\}$ the imaginary part of a complex number.

Let the H matrix in (3) be

$$H = \begin{bmatrix} 1 & 0 & \xi_2 \cos \phi_2 & \xi_2 \sin \phi_2 \\ 0 & 1 & -\xi_2 \sin \phi_2 & \xi_2 \cos \phi_2 \\ \xi_1 \cos \phi_1 & \xi_1 \sin \phi_1 & 1 & 0 \\ -\xi_1 \sin \phi_1 & \xi_1 \cos \phi_1 & 0 & 1 \end{bmatrix} \quad (7)$$

which is isomorphic to the complex matrix

$$A = \begin{bmatrix} 1 & \xi_2 e^{j\phi_2} \\ \xi_1 e^{j\phi_1} & 1 \end{bmatrix} \quad (8)$$

utilized in [2].

In (7), ξ_2 is the coupling coefficient from $S_1(t)$ to $S_2(t)$ and ϕ_2 is a random variable that is uniform in $[0, 2\pi]$. Also, (ξ_1, ϕ_1) represents the coupling from $S_2(t)$ to $S_1(t)$. Note that the form H in (7) excludes cross-rail interference between the real and imaginary components of each signal. The variations of all the coupling parameters are assumed to be very slow such that, over the short memory of an optional interleaver introduced after the convolutional encoder, these parameters do not change. The interleaver is used to make sure that the coded interfering symbols are independent. This is the system that we analyze. In practice we believe that the interleaver is not necessary, and that the performance of the system is close to the results of this paper.

In the case when compensation for cross-coupling is not involved in the receiver, system performance can be determined from (4)–(7). When such compensation is used we must proceed as follows.

A system block diagram is given in Fig. 1. As a compensator for cross-coupled interference, we shall use the “diagonalizer” from [2]. This compensator removes the cross-coupling between the two QAM signals $S_1(t)$ and $S_2(t)$. However, through its zero-forcing of the cross-coupled signal, it enhances the noise and introduces cross-rail interference into each of the real and imaginary components of the QAM signals. Our chief purpose is to analyze the performance of trellis coding in the presence of this residual interference, and also the cross-coupling interference when no compensation is adopted. In practice the minimum mean-square error (MMSE) canceler from [2] would probably be a more suitable compensator as, for uncoded transmission, its performance is superior to the diagonalizer. Although the MMSE canceler can be analyzed, the notation is too cumbersome.

To model the diagonalizer from [2] we form RW , with R as in (3), and the purpose of W is to make HW become a matrix of the form

$$HW = \begin{bmatrix} \cdot & \cdot & 0 & 0 \\ \cdot & \cdot & 0 & 0 \\ 0 & 0 & \cdot & \cdot \\ 0 & 0 & \cdot & \cdot \end{bmatrix} \quad (9)$$

and, as such, remove the complex signal cross-coupling. For H as in (7) it turns out that

$$W = \begin{bmatrix} 1 & 0 & -\xi_2 \cos \phi_2 & -\xi_2 \sin \phi_2 \\ 0 & 1 & \xi_2 \sin \phi_2 & -\xi_2 \cos \phi_2 \\ -\xi_1 \cos \phi_1 & -\xi_1 \sin \phi_1 & 1 & 0 \\ \xi_1 \sin \phi_1 & -\xi_1 \cos \phi_1 & 0 & 1 \end{bmatrix} \quad (10)$$

gives HW of the form in (9). The signal values for data detection ($\tilde{R} = RW$) are then

$$\tilde{R} = DHW + NW \quad (11)$$

and system performance can readily be determined from (3)–(7) and, also, (10) and (11). We first consider the case for uncoded transmission.

III. PERFORMANCE FOR THE UNCODED CASE

A. No Compensation

For the case of no interference compensation and no channel coding of the data vector D in (5), the system error probability follows from a consideration of (3). The estimate of δ_{1k} in (5) is given by the first component of R in (3):

$$\hat{\delta}_{1k} = \delta_{1k} + \xi_1 \cos \phi_1 \delta_{2k} - \xi_1 \sin \phi_1 \beta_{2k} + n_{1R} \quad (12)$$

where n_{1R} is a sample of a zero-mean, Gaussian random process with variance σ^2 . For ease of notation we drop the sampling instant parameter in our noise samples, which are uncorrelated. Then, as the signal points are separated by $2C$ units,

$$\begin{aligned} P(e|\phi_1, \beta_{2k}, \delta_{2k}) &= P\{|Y + n_{1R}| > C\} \\ &= \frac{2(L-1)}{L} Q\left(\frac{C-Y}{\sigma}\right) \end{aligned} \quad (13)$$

where

$$Y = \xi_1 \cos \phi_1 \cdot \delta_{2k} - \xi_1 \sin \phi_1 \cdot \beta_{2k} \quad (14)$$

and $Q(x) = (1/\sqrt{2\pi}) \int_x^{\infty} e^{-\eta^2/2} d\eta$.

The result in (13) is the symbol error probability conditioned on $(\phi_1, \beta_{2k}, \delta_{2k})$ for a prescribed value of the cross-coupling coefficient, ξ_1 . The unconditioned symbol error

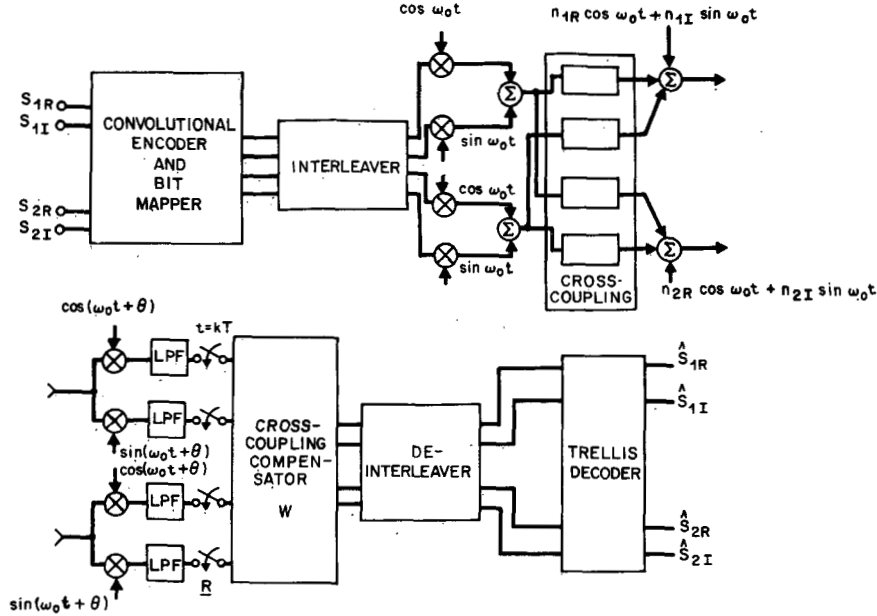


Fig. 1. System model.

probability is determined from the moments of the random variable Y in (14). Now the signal-to-noise ratio for noncross-coupled M -ary QAM is

$$\gamma_0 = \frac{(L^2 - 1)C^2}{3\sigma^2} = 2 \frac{E_b}{N_0} \log_2(L) \quad (15)$$

where E_b is the energy per information bit, L^2 is the number of signal points, and N_0 is the one-sided spectral height of additive white Gaussian noise. Thus,

$$P(e|\phi_1, \beta_{2k}, \delta_{2k}) = \frac{2(L-1)}{L} Q \left(\sqrt{\frac{3\gamma_0}{L^2-1}} (1-Y') \right) \quad (16)$$

where $Y' = Y/C$, the normalized value of Y in (14). Using the method of moments (see [8] or [9, Appendix C]), we have

$$P(e) = \frac{2(L-1)}{L} \sum_j w_j Q \left(\sqrt{\frac{3\gamma_0}{L^2-1}} (1-\zeta_j) \right) \quad (17)$$

where (w_j, ζ_j) are the weights and nodes for the random variable Y' . The parameters (w_j, ζ_j) are determined from the moments of Y' and these moments are derived in the Appendix.

B. Compensator Analysis

In presence of the compensator, the decision variable can be chosen from the first component of \hat{R} in (11). Use of (7)-(11) results in

$$\begin{aligned} \hat{R}_1 = & \delta_{1k} - \xi_1 \xi_2 \delta_{1k} \cos \phi + \xi_1 \xi_2 \beta_{1k} \sin \phi \\ & + n_{1R} + n_{2I} \xi_1 \sin \phi_1 - n_{2R} \xi_1 \cos \phi_1 \end{aligned} \quad (18)$$

where $\phi = \phi_1 + \phi_2$. Use of the normalization

$$\delta_{1k} = \frac{\hat{R}_1}{1 - \xi_1 \xi_2 \cos \phi} \quad (19)$$

gives the symbol error probability, conditioned on (ϕ, β_{1k}) , as

$$P(e|\phi, \beta_{1k}) = \frac{2(L-1)}{L} Q \left(\frac{C-\Delta}{\sigma_n} \right) \quad (20)$$

where $\Delta = \xi_1 \xi_2 \beta_{1k} \sin \phi (1 - \xi_1 \xi_2 \cos \phi)^{-1}$ and

$$\sigma_n^2 = \frac{\sigma^2(1 + \xi_1^2)}{(1 - \xi_1 \xi_2 \cos \phi)^2} \quad (21)$$

In terms of E_b/N_0 we have

$$\begin{aligned} P(e|\phi, \beta_{1k}) &= \frac{2(L-1)}{L} Q \left(\sqrt{\frac{6E_b \log_2 L}{N_0(L^2-1)(1+\xi_1^2)}} (1-Z') \right) \end{aligned} \quad (22)$$

where $Z' = Z/C$ and

$$Z = \xi_1 \xi_2 [\cos \phi - \beta_{1k} \sin \phi]. \quad (23)$$

We note that the normalization in (19) is easily accomplished in practice by using an automatic gain control (AGC) device. The moments of Z in (23) are derived in the Appendix.

IV. COMBINED MODULATION AND CODING

A. Modulation/Coding Specification

Ungerboeck demonstrated in [3] that very efficient combined channel coding and modulation schemes are obtained by combining convolutional codes with, e.g., multilevel amplitude modulation (AM) in one or two dimensions. He found that simple rate $m/(m+1)$ codes for signal sets with $2^{(m+1)}$ signal points performed quite well when the mapping rule (i.e., the binary word associated with each signal point) and the convolutional codes are selected following certain design rules. Typically only a few of the incoming m bits per signal point are actually coded. The "most significant" bits in the mapper word are not encoded. Thus, the actual encoder that needs to be found is a rate $\bar{m}/(\bar{m}+1)$ where \bar{m} is often 1 or 2; see [3]-[5], [7]. The overall rate is $m/(m+1)$, leaving $m - \bar{m}$ uncoded information bits. The receiver consists of a Viterbi detector that compares the received signal to all possible transmitted signals without interference.

Briefly, to get the error event probability with or without coding, let \mathbf{R} be the received signal vector, s_i and s_j , $i \neq j$, be two competing signals, and consider s_i as transmitted. An error event occurs when

$$\|\mathbf{R} - s_i\|^2 > \|\mathbf{R} - s_j\|^2 \quad (24)$$

where $\|s\|^2$ is the squared Euclidean distance of s . Now assume $\mathbf{R} = s_i + \mathbf{N} + \mathbf{I}$ where \mathbf{N} is the Gaussian noise vector and \mathbf{I} is the interference vector. Then an error event is defined as

$$\left\{ x_s = \mathbf{N} \cdot \frac{\Delta s}{d_{ij}} > \frac{d_{ij}}{2} - \mathbf{I} \cdot \frac{\Delta s}{d_{ij}} \right\} \quad (25)$$

with $d_{ij}^2 = \|\Delta s\|^2$ and $\Delta s = s_j - s_i$. Now the components of vector \mathbf{N} are all Gaussian and independent with zero-mean and variance σ_n^2 . Hence, x_s is zero-mean Gaussian with variance σ_n^2 . Thus, the probability of an error event conditioned on the interference vector \mathbf{I} is

$$P(\text{error event} | \mathbf{I}) = Q\left(\frac{d_{ij} - \mathbf{I} \cdot \Delta s}{2\sigma_n} - \frac{\mathbf{I} \cdot \Delta s}{\sigma_n d_{ij}}\right). \quad (26)$$

We now use the previous results for evaluation of the error event probability for various coding methods. The moment method [8], [9] is used to average the error event probability with respect to the interference vector \mathbf{I} in (26). Earlier [10], [11] bounds were used to estimate the error probability, but the moment method is felt to be more precise.

The Viterbi detection of trellis coded modulation is described in, for example, [12]–[15]. There are two types of error events that are particularly important for the design and analysis of trellis coded modulation. The first type consists of parallel transitions. These are of length one channel symbol time and have errors only among the uncoded bits. The second type are typically longer and always have errors among the coded bits. The parallel transition error events occur for any transmitted signal point and for any point in time, independently, from symbol to symbol. The optimum codes for the Gaussian channel often have the property that the Euclidean distance between signals corresponding to parallel transitions, d_p^2 , is larger than the overall minimum Euclidean distance for the combined coding and modulation scheme. The minimum distance is then given by the second type of error event, namely, an error event corresponding to two different coded paths among the coded bits of the mapper word. We will denote the minimum normalized squared Euclidean distance among all coded events as d_c^2 . By increasing the code memory (i.e., the number of code states), d_c^2 can be increased. By increasing \bar{m} , the minimum squared normalized Euclidean distance between parallel transitions d_p^2 can be increased. The overall minimum distance of the coded modulation scheme is $d_{\min}^2 = \min(d_p^2, d_c^2)$.

The above distance considerations are all based on the assumption that coherent transmission occurs on an ideal additive white Gaussian channel. Below we will consider analysis in the presence of interference for the codes initially constructed for the ideal Gaussian channel.

Figs. 2 and 3 show examples of coded AM and QAM schemes considered in this paper. In Fig. 2 the modulation is eight-level AM and the code is a rate 1/2 code on two of the 3 bits. In Fig. 3 the code memory is $v = 2$, the number of coded bits is $\bar{m} = 2$, and the modulation is 16-QAM. The mapper is the one given in [15]. The performance analyses of other coded QAM and AM schemes are given in [15].

Although the parallel transition dominates the distance for the memory $v = 2$ code in Fig. 3, the next minimum distance affects the error probability for low and intermediate signal-to-noise ratios for the Gaussian channel (without interference).

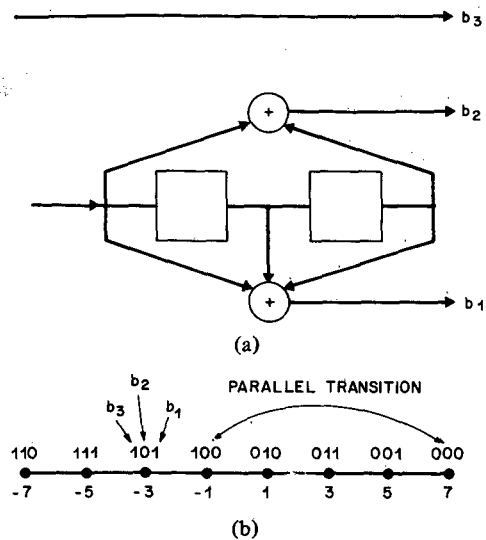


Fig. 2. (a) Rate 2/3 encoder with 1 bit uncoded. (b) Symbol mapping by set partitioning, 8-AM.

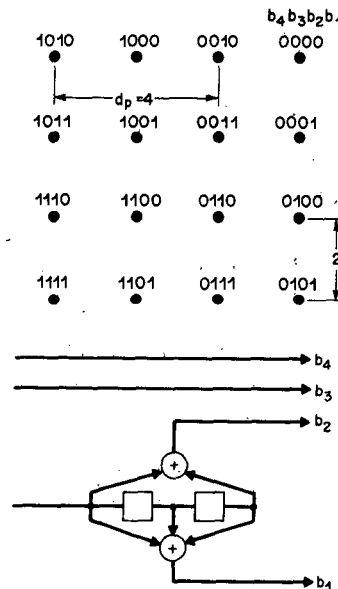


Fig. 3. Example of mapper and $v = 2$ coder where a rate 1/2 code is used and where the parallel transitions corresponding to the uncoded bits dominate the minimum distance. The overall rate of the coded 16-QAM system is 3/4.

As we will see below, it will be even more important to study error events of different lengths and distances for the interference case. For the case of coding on two rails, the difference signal vector is defined as $\Delta s = (a_1, b_1, a_2, b_2, a_3, b_3, \dots, a_k, b_k, \dots)$ where a_k and b_k are the components of Δs in the in-phase and quadrature rails at time k , respectively.

For the memory $v = 2$ code in Fig. 3, the next minimum distance event has the squared normalized distance of 20. This corresponds to the difference signal vector $\Delta s = \{2, 2, 0, 2, 2, 2\}$ while the minimum squared distance is 16, given, e.g., by $\Delta s = \{4, 0\}$ or $\Delta s = \{0, 4\}$ parallel transitions.

B. Performance Analysis: No Compensation

From the channel model it now follows that the decision variables for the received symbols corresponding to S_{1R} and S_{1I} rails are

$$\begin{cases} \delta_{1k} = \delta_{1k} + \xi_1 \delta_{2k} \cos \phi_1 - \xi_1 \beta_{2k} \sin \phi_1 + n_{1R} \\ \beta_{1k} = \beta_{1k} + \xi_1 \delta_{2k} \sin \phi_1 + \xi_1 \beta_{2k} \cos \phi_1 + n_{1I} \end{cases} \quad (27)$$

TABLE I
THE EFFECT OF WORST CASE INTERFERENCE FOR TWO-RAIL CODING
WITHOUT INTERFERENCE COMPENSATION WHERE THE CODING IS
DONE IN THE SAME QAM CONSTELLATION, S_{1R} , S_{1I} , (X'_{\max}) AND
THE EFFECT OF WORST CASE INTERFERENCE FOR TWO-RAIL
CODING WITHOUT INTERFERENCE COMPENSATION WHERE
THE CODING IS PERFORMED ON RAILS IN DIFFERENT
QAM CONSTELLATIONS, S_{1R} , S_{2I} , (A_{\max} , B_{\max})

SCHEME	ERROR EVENT	d_{12}^2	X'_{\max}	A_{\max}	B_{\max}
UNCODED 16-QAM	(2,0)	4	$3\sqrt{2} \approx 4.24$	$3\sqrt{2} \approx 4.24$	$3\sqrt{2} \approx 4.24$
UNCODED 8-AMPM	(2,2)	8	3	$3\sqrt{2} \approx 4.24$	$1.5\sqrt{2} \approx 2.12$
CODED 16-QAM	(4,4)	32	1.5	$1.5\sqrt{2} \approx 2.12$	$1.5\sqrt{2} \approx 1.06$
CODED 16-QAM	(4,0)	16	$1.5\sqrt{2} \approx 2.12$	$1.5\sqrt{2} \approx 2.12$	$1.5\sqrt{2} \approx 2.12$
CODED 16-QAM	(2,2,0,2,2,2)	20	$0.6(4 + \sqrt{2}) \approx 3.25$	$3\sqrt{2} \approx 4.24$	$1.2\sqrt{2} \approx 1.69^*$

* Alternatively $1.8\sqrt{2} \approx 2.55$ depending on mapping, since the error event is slightly unsymmetric with respect to the in-phase and quadrature components.

for each signal point δ_{1k} , β_{1k} at time k . Using the technique described earlier, we have the conditional error event probability

$$P(\text{error event} | \phi_1, \{\delta_{2k}, \beta_{2k}\})$$

$$= Q \left(d_{ij} \sqrt{\frac{3r_c E_b \log_2 L}{2N_0(L^2 - 1)}} (1 - X) \right) \quad (28)$$

where

$$X = \frac{2\xi_1}{d_{ij}^2} \left\{ \cos \phi_1 \sum_k (a_k \delta_{2k} + b_k \beta_{2k}) - \sin \phi_1 \sum_k (a_k \beta_{2k} - b_k \delta_{2k}) \right\} \quad (29)$$

where the summation over the k 's is taken over the components of the difference vector, a_k , b_k corresponding to the error event; and r_c is the overall rate of the coded system. Thus, the error event probability is conditioned on interference components corresponding to all components of the error event. The average error event probability is obtained by averaging (28) over ϕ_1 and $\{\delta_{2k}, \beta_{2k}\}$ assuming a uniform distribution of ϕ_1 and independent interfering symbols $\{\delta_{2k}, \beta_{2k}\}$ with a uniform distribution.

It is immediately clear from (29) that there is a worst case combination of phase ϕ_1 and interfering data symbols $\{\delta_{2k}, \beta_{2k}\}$. This worst case parameter combination will dominate the average error event probability for high signal-to-noise ratio values. By determining this worst case we will establish guidelines and bounds for the error probability behavior of the uncoded and the coded schemes. The worst case of the error event probability in (28) can be expressed as

$$P(\text{error event} | \text{worst case parameter combination})$$

$$= Q \left(d_{ij} \sqrt{\frac{3r_c E_b \log_2 L}{2N_0(L^2 - 1)}} (1 - X_{\max}) \right) \quad (30)$$

where

$$X_{\max} = \xi_1 X'_{\max} = \xi_1 \text{Max}_{\phi_1, \delta_{2k}, \beta_{2k}} \frac{2}{d_{ij}^2} \left[\cos \phi_1 \sum_k (a_k \delta_{2k} + b_k \beta_{2k}) - \sin \phi_1 \sum_k (a_k \beta_{2k} - b_k \delta_{2k}) \right] \quad (31)$$

It is reasonably straightforward to derive Table I for some of the cases which are of interest to us, namely uncoded 16-QAM, uncoded 8-AMPM used in [3], and coded 16-QAM. From the data in Table I the relative asymptotic error probability behavior of each error event can be calculated. For $\xi_1 X'_{\max} < 1$, the degradation in channel signal-to-noise ratio in decibels relative to the case of no interference is $10 \log_{10} (1 - \xi_1 X'_{\max})^2$ dB, and the relative degradation compared to the minimum distance error event for the case of no interference is

$$10 \cdot \log_{10} \left(\frac{d_{ij}^2 (1 - \xi_1 X'_{\max})^2}{d_{\min}^2} \right) \text{ dB.} \quad (32)$$

From Table I we can also derive the value of ξ_1 for which there is a "floor" on the error probability curve. This happens when ξ_1 is large enough to yield a worst case interference vector that brings the decision variables on the "wrong" side of the decision boundary, i.e., $\xi_1 X'_{\max} > 1$. Thus, for this parameter combination an erroneous decision will be made even for infinitely high E_b/N_0 values. For uncoded 16-QAM, a floor will start appearing for $\xi_1 > 1/3\sqrt{2}$. The corresponding values of ξ_1 can easily be calculated for the other schemes.

C. Diversity: No Compensation

We will now analyze the error event probability for coded QAM where the transmission of the coded in-phase component is done over one QAM constellation and the transmission of the coded quadrature component is done over the other QAM constellation. The decision variables in this case are

$$\begin{cases} \delta_{1k} = \delta_{1k} + \xi_1 \delta_{2k} \cos \phi_1 - \xi_1 \beta_{2k} \sin \phi_1 + n_{1R} \\ \beta_{2k} = \beta_{2k} + \xi_2 \delta_{1k} \sin \phi_2 + \xi_2 \beta_{1k} \cos \phi_2 + n_{2I} \end{cases} \quad (33)$$

Equation (33) should be compared with (27), which was for no diversity. In the previous section the average error event probability was calculated by first calculating the error event probability conditioned on the interference. In the present case there is one more complication, that is, the interference vector is now a function of the transmitted signal.

Proceeding as in our earlier analysis,

$$P(\text{error event} | \phi_1, \phi_2, \{\delta_{1k}, \beta_{2k}, \delta_{2k}, \beta_{1k}\}) \\ = Q \left(\sqrt{\frac{3r_c E_b \log_2(L)}{2N_0(L^2-1)}} d_{ij}(1-X) \right) \quad (34)$$

where

$$X = \frac{2}{d_{ij}^2} \left\{ \xi_1 \sum_k a_k [\delta_{2k} \cos \phi_1 - \beta_{2k} \sin \phi_1] \right. \\ \left. + \xi_2 \sum_k b_k [\delta_{1k} \sin \phi_2 + \beta_{1k} \cos \phi_2] \right\}. \quad (35)$$

Note that δ_{1k}, β_{2k} are now the transmitted sequence and δ_{2k}, β_{1k} are the interfering symbols. The average of (34) is calculated with the method of moments for a given data sequence, in particular the worst case sequence, as will be seen in the numerical results section.

The worst case of (35) has been calculated for some interesting scenarios using the same method as before. The worst case of $X < 1$ is now calculated for the worst interference parameters and the worst transmitted sequence. In particular, we will consider the two limiting cases of $\xi_1 = \xi_2$ (same interference) and $\xi_2 = 0$ (only coupling in one direction). For the two cases, for $\xi_1 = \xi_2$, we have $X_{\max} = \xi_1 A_{\max} = \xi_2 A_{\max}$, and for the case where $\xi_2 = 0$ we have $X_{\max} = \xi_1 B_{\max}$. Thus, we obtain the results shown in Table I. Study of the results in Table I shows that the worst case with $\xi_1 = \xi_2$ is worse than X'_{\max} (A_{\max} is larger). On the other hand, for the schemes with error events having components on both rails, B_{\max} is smaller than both A_{\max} and X'_{\max} . Thus, for all error events we have $A_{\max} \geq X'_{\max}$ and $B_{\max} \leq X'_{\max}$.

D. Performance Analysis: With Compensation

We now consider combined QAM and convolutional coding on channels with compensated interference. Using the channel model with compensation, we obtain the decision variables

$$\delta_{1k} = \delta_{1k} + \frac{\xi_1 \xi_2 \sin \phi}{1 - \xi_1 \xi_2 \cos \phi} \beta_{1k} + \frac{1}{1 - \xi_1 \xi_2 \cos \phi} \\ \cdot (n_{1R} - n_{2R} \xi_1 \cos \phi_1 + n_{2I} \xi_1 \sin \phi_1) \quad (36)$$

$$\beta_{1k} = \beta_{1k} + \frac{\xi_1 \xi_2 \sin \phi}{1 - \xi_1 \xi_2 \cos \phi} \delta_{1k} + \frac{1}{1 - \xi_1 \xi_2 \cos \phi} \\ \cdot (n_{1I} - n_{2R} \xi_1 \sin \phi_1 - n_{2I} \xi_1 \cos \phi_1) \quad (37)$$

where k denotes the successive signal points in the QAM constellation. Again, using similar arguments as before, we obtain

$$P(\text{error event} | \phi_1, \phi_2, \{\delta_{1k}, \beta_{1k}\}) \\ = Q \left(\sqrt{\frac{3r_c E_b \log_2(L)}{2N_0(L^2-1)}} \frac{d_{ij}}{\sqrt{1 + \xi_1^2}} (1-X) \right) \quad (38)$$

with

$$X = \xi_1 \xi_2 \left[\cos \phi - \frac{2 \sin \phi}{d_{ij}^2} \sum_k (a_k \beta_{1k} + b_k \delta_{1k}) \right] \quad (39)$$

where $\phi = \phi_1 + \phi_2$. With the method of moments, the average of (39) over ϕ is calculated conditioned on any transmitted sequence and in particular for the worst case sequences.

The worst case error probability for $X_{\max} < 1$ is given by $X_{\max} = \xi_1 \xi_2 X'_{\max}$ where X'_{\max} is minimized over ϕ for the worst case (δ_{1k}, β_{1k}) for any given error event. The asymptotic degradation for any error event with distance d_{ij}^2 due to interference is $10 \log_{10} ((1 - \xi_1 \xi_2 X'_{\max})^2 / (1 + \xi_1^2))$ dB, and the asymptotic degradation due to interference, compared to the performance with no interference, is $10 \log_{10} (d_{ij}^2 (1 - \xi_1 \xi_2 X'_{\max})^2 / d_{\min}^2 (1 + \xi_1^2))$ dB. Straightforward maximizations yield the worst case results in Table II. From this table we can, for example, see that the error probability "floor" occurs for the same value of the product $\xi_1 \xi_2$ for uncoded 16-QAM, 8-AMPM, and the next minimum distance error event for the memory $\nu = 2$ coded 16-QAM scheme.

It is clear from the error event formulas that for any given error event, a sufficiently large interference level will make $X_{\max} > 1$ and, consequently, cause a floor in the error probability. Thus, errors can occur even if there is no Gaussian noise. By examining the expressions for the error probability, we can conclude that there is a worst case type of error event which will maximize X_{\max} and, thus, will be the first error event that will have a worst case error probability which is irreducible for high signal-to-noise ratios. However, even for very long error events there are maximum values of ξ_1 and ξ_2 for which the error probability does not have a floor. We will now identify these worst case error events for the cases considered above.

In general, no coded error event (even infinitely long) will have X'_{\max} larger than the uncoded X'_{\max} for the same signal set. For example, for coded 16-QAM, assume a hypothetical error event which is of length $2K$ where the Δs is $(2, 0, 2, 0, 2, 0, \dots, 2, 0)$. Straightforward calculations show that $X'_{\max} = 3\sqrt{2}$ in Table I and $X'_{\max} = \sqrt{10}$ in Table II. These values are independent of K . It is apparent that the above hypothetical error event of length $2K$ is the one that maximizes X'_{\max} . Thus, an upper bound on ξ_1 and ξ_2 can be established below which none of the error event probabilities will have a floor.

E. Diversity: With Compensation

Coding after interference compensation can also be analyzed when two different QAM signal constellations are used. In this case the conditional error probability is

$$P(\text{error event} | \phi_1, \phi_2, \{\delta_{2k}, \beta_{1k}\}) \\ = Q \left(\sqrt{\frac{3r_c E_b \log_2(L)}{2N_0(L^2-1)}} \cdot \frac{d_{ij}}{\sqrt{1 + \frac{1}{2}(\xi_1^2 + \xi_2^2)}} \cdot (1-X) \right) \quad (40)$$

with

$$X = \xi_1 \xi_2 \left[\cos \phi - \frac{2 \sin \phi}{d_{ij}^2} \sum_k (a_k \beta_{1k} + b_k \delta_{2k}) \right] \quad (41)$$

In this case the average of P in (40) over $\phi_1, \phi_2, \delta_{2k}, \beta_{1k}$ can be calculated by the method of moments. The worst case behavior of (41) is given by the X'_{\max} values, which are the same as those in Table II. The relative asymptotic degradation compared to interference-free transmission for an error event with distance d_{ij}^2 is now

$$10 \log_{10} \left(\frac{d_{ij}^2 (1 - \xi_1 \xi_2 X'_{\max})^2}{d_{\min}^2 \left(1 + \frac{1}{2} (\xi_1^2 + \xi_2^2) \right)} \right) \text{ dB}. \quad (42)$$

TABLE II
THE EFFECT OF WORST CASE INTERFERENCE FOR TWO-RAIL CODING WITH INTERFERENCE COMPENSATION WHERE THE CODING IS PERFORMED ON RAILS IN THE SAME QAM CONSTELLATION

SCHEME	ERROR EVENT	d_{12}^2	X'_{\max}
UNCODED 16-QAM	(2,0)	4	$\sqrt{10} \approx 3.16$
UNCODED 8-AMPM	(2,2)	8	$\sqrt{10} \approx 3.16$
CODED 16-QAM	(4,4)	32	$\frac{\sqrt{13}}{2} \approx 1.803$
CODED 16-QAM	(4,0)	16	$\frac{\sqrt{13}}{2} \approx 1.803$
CODED 16-QAM	(2,2,0,2,2,2)	20	$\sqrt{10} \approx 3.16$

TABLE III
THE EFFECT OF WORST-CASE INTERFERENCE ON CODING GAIN FOR ONE-RAIL CODING WITHOUT (Y'_{\max}) AND WITH INTERFERENCE COMPENSATION (Z'_{\max})

SCHEME	ERROR EVENT	d_{12}^2	Z'_{\max}	Y'_{\max}
UNCODED 4-AM	2	4	≈ 3.16	$3\sqrt{2} = 4.24$
UNCODED 8-AM	2	4	≈ 7.07	$7\sqrt{2} = 9.90$
CODED 8-AM	4,2,4	36	≈ 4.01	≈ 5.50
CODED 8-AM	4,2,0,2,4	40	≈ 4.32	≈ 5.94

By comparing (40) and (41) to (38) and (39), we note that they coincide for the case $\xi_1 = \xi_2$. Furthermore, for $\xi_2 < \xi_1$ there is a small advantage to be gained, as can be seen from (42). However, for desired parameter combinations this advantage is only a small fraction of a decibel.

F. Other Signal Sets

It is straightforward to modify the above technique to coded AM. Table III shows the equivalent of Tables I and II for coded 8-AM and uncoded 4-AM with compensation (Y'_{\max}) and without compensation (Z'_{\max}). In the numerical result section we will discuss the performance of the code in Fig. 2. The diversity concept considered herein is not applicable to one-dimensional AM.

V. NUMERICAL RESULTS

We have calculated the error event probability for the shortest dominating error events for the combined convolutional codes and multilevel AM and QAM schemes described earlier. For comparison, the performance of 4-AM, 16-QAM, and 8-AMPM without coding have also been evaluated. All schemes are considered with and without interference compensation.

A. No Interference Compensation

Fig. 4 shows the average symbol error probability for uncoded 16-QAM without coding and interference compensation. The interference coupling parameter ξ_1 is varied, and on the curves, $10 \log_{10}(\xi_1^2)$ is displayed in decibels. The behavior of these curves is well matched to the results for the worst case

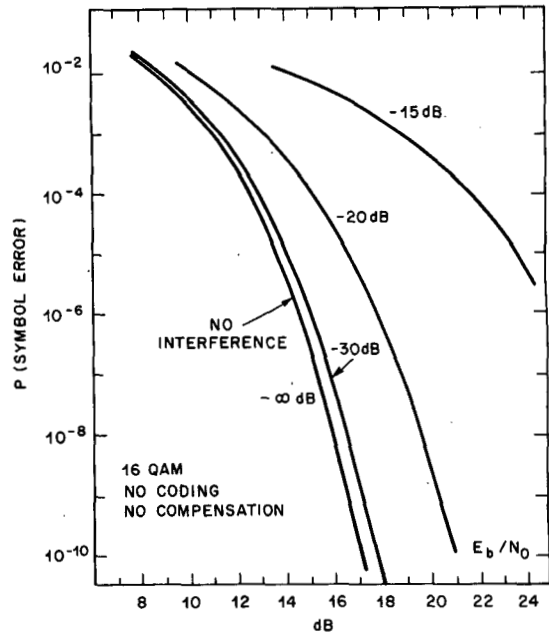


Fig. 4. Average symbol error probability versus E_b/N_0 for uncoded 16-QAM. No interference compensation is used. The coupling parameter ξ_1 is shown in decibels ($10 \log_{10} \xi_1^2$).

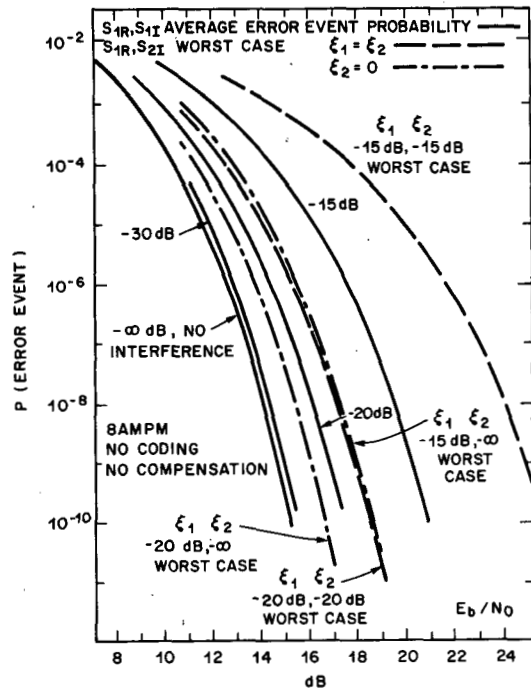


Fig. 5. Average error event probability for 8-AMPM for the S_{1R}, S_{1I} case for different values of ξ_1 (solid curves) and worst case error event probability for the S_{1R}, S_{2I} case with $\xi_1 = \xi_2$ and for some values of ξ_1 when $\xi_2 = 0$.

analysis presented in Table I. Uncoded 8-AMPM without interference compensation has also been analyzed. The results are shown in Fig. 5 and should be compared to the data in Table I. By comparing the average error probability curves in Fig. 4 and 5, we observe that 8-AMPM suppresses interference more effectively than 16-QAM. This is also consistent with the worst case comparisons in Table I. Fig. 5 also shows the result when 8-AMPM signals are transmitted by means of the in-phase rail over one constellation using channel 1 and the quadrature component over the other constellation using

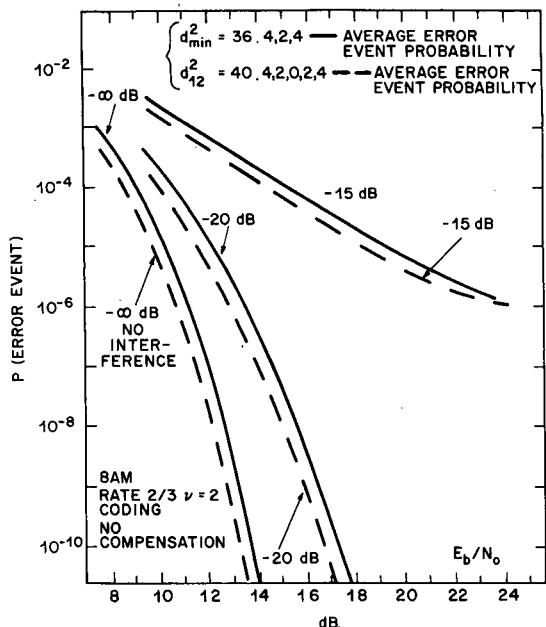


Fig. 6. Average error event probability for the minimum and next minimum distance error event for $\nu = 2$, rate 2/3 coded 8-AM without interference compensation. For comparison, 4-AM with interference is shown in Fig. 4.

channel 2. In this case we have only analyzed the average error event probability for the worst transmitted sequence for the two limiting cases with $\xi_1 = \xi_2$ and with $\xi_2 = 0$. These cases are referred to as (S_{1R}, S_{2I}) worst case in Fig. 5. Note that the worst case with $\xi_2 = 0$ is much better than the average error event probability for the case when both the in-phase and the quadrature components are transmitted in the same constellation over the same channel. On the other hand, the two-channel case with $\xi_1 = \xi_2$ exhibits results worse than the average error event probability when both the in-phase and quadrature rails of one signal are transmitted over the same channel. This was to be expected from the results in Table I.

Coding on one rail with eight-level AM and a rate 1/2, memory $\nu = 2$ on two of the 3 bits yields the error event probabilities shown in Fig. 6. Comparison of these results to uncoded 4-AM, shown in Fig. 4, seems to indicate that the coding gain obtained for the interference-free channel is maintained for low interference levels; however, it is not increased. Compare these results to the worst case results in Table III. The average error event probabilities in Fig. 6 and the results in Table III are quite consistent.

Results for the coded 16-QAM scheme are shown in Fig. 7. Error event probabilities for the minimum distance parallel transition ($d_p^2 = 16$) and the next minimum distance (long) error event are shown. The coding gain compared to uncoded 16-QAM and also to the uncoded 8-AMPM now seems to be increased for "reasonable" intermediate interference levels compared to the gain for no interference. Notice the difference between the one-rail code in Fig. 6 and the coded 16-QAM scheme in Fig. 7. Also compare the results in Fig. 7 to the data in Table I. Note that the minimum distance error event dominates the other error events for low values of the error probability and ξ_1 . However, for ξ_1 at -15 dB, the error event probability for the next minimum distance error event becomes larger than that for the minimum distance (parallel transition) error event. This trend is even more apparent for -10 dB interference level. These results are in good agreement with the results in Table I.

Fig. 8 indicates the potential diversity properties of transmitting coded 16-QAM over in-phase and quadrature rails in two different constellations. We have analyzed the

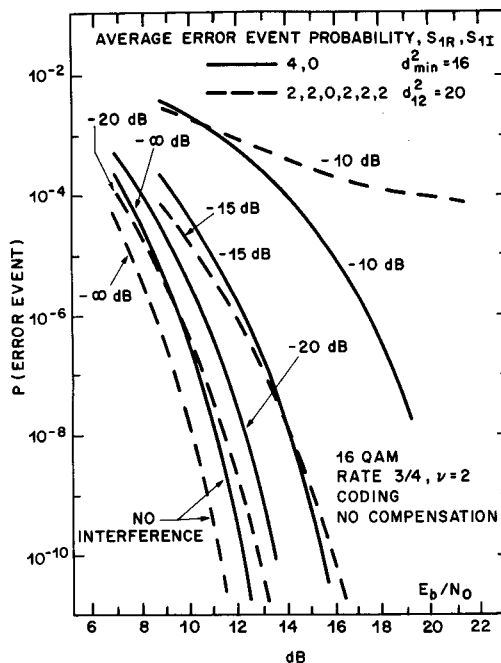


Fig. 7. Average error event probability for the minimum and the next minimum distance error event for the $\nu = 2$, rate 3/4 coded 16-QAM without interference compensation. The two coded QAM rails are transmitted over the same channel, S_{1R}, S_{1I} .

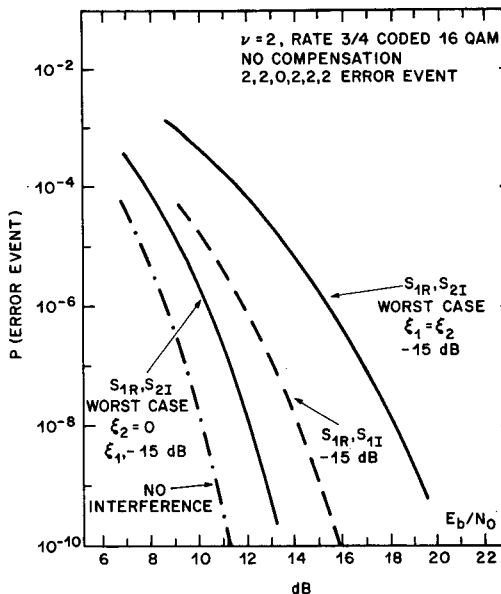


Fig. 8. Worst case error event probability for the next minimum distance error event for the S_{1R}, S_{2I} case both for $\xi_1 = \xi_2$ at -15 dB and for $\xi_2 = 0$, ξ_1 at -15 dB. Compare the average error event probability for the S_{1R}, S_{1I} case with ξ_1 at -15 dB.

average error event probability for the worst transmitted sequence, denoted (S_{1R}, S_{2I}) worst case in the figure for the two limiting cases of $\xi_1 = \xi_2$ and $\xi_2 = 0$ for proper parameter combinations. Fig. 8 is representative of these results. For the particular error event shown, we can see that the worst case $\xi_2 = 0$ is significantly better, than the average error event probability for the case where the coded in-phase and quadrature rails are transmitted over the same constellation. On the other hand, the worst case error event probability for the $\xi_1 = \xi_2$ case and different QAM constellations is significantly worse. These trends seem to match those

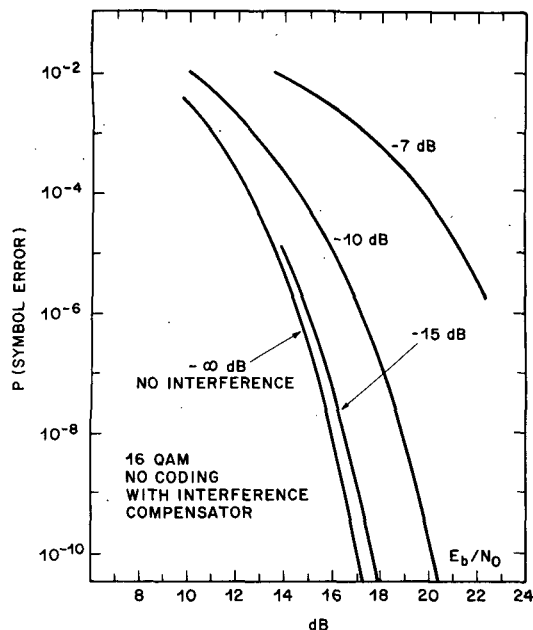


Fig. 9. Average symbol error probability of uncoded 16-QAM. Interference compensator is used.

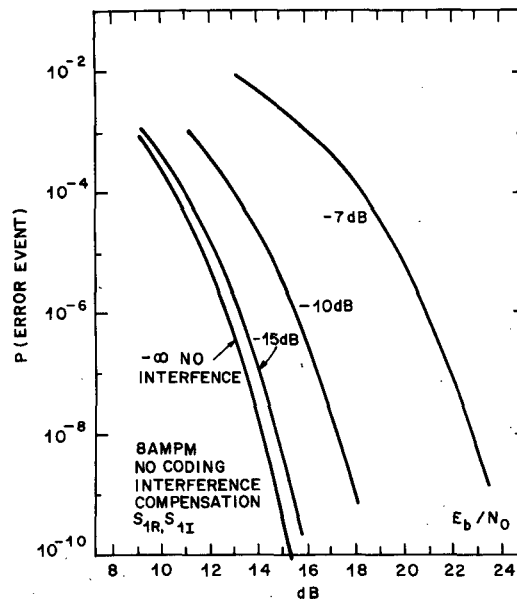


Fig. 10. Worst case error event probability for uncoded 8-AMPM for transmission of both rails over one channel (S_{1R} , S_{1I}). Interference compensation is used.

indicated in Table I. Whether any overall gain in system performance is achieved by sending the coded I and Q rails over different QAM constellations depends on the distribution of ξ_1 and ξ_2 . It is, however, clear from Table I that with $\xi_1 = \xi_2$, there is no gain by coding over two constellations. On the contrary, Table I clearly indicates that it is better to use only one constellation. When one of ξ_1 or ξ_2 is small, we obtain diversity gains compared to the worst of the QAM channels. *This could be exploited, for example, in dual-polarized microwave radio channels.* If the polarized signals are subject to independent fades and, as a result, independent cross-coupling factors, joint coding can provide diversity and, as a result, a larger overall system throughput.

B. With Interference Compensation

Figs. 9 and 10 show the performance of uncoded 16-QAM and 8-AMPM, respectively, when the diagonalizer considered in (10) is utilized. Fig. 9 shows the average symbol error probability for 16-QAM and Fig. 10 shows the worst case symbol error event probability for 8-AMPM calculated for the case of one constellation and for the case of $\xi_1 = \xi_2$. The average is slightly better and the relative difference between the curves for 8-AMPM is very similar to that for 16-QAM. This is consistent with Table II. Notice the difference compared to Figs. 4 and 5, which are for the case of no compensation. It is clear that compensation is effective.

Fig. 11 shows the average error event probability for coded 8-AM, memory $\nu = 2$ coding on one rail and with an interference compensator. Comparing this figure to uncoded 4-AM (16-QAM, Fig. 9), we can see that there seems to be some interference suppression with this code, but not very much. Fig. 11 also shows some worst case error event probability values where in the derivation we have chosen the worst case interfering symbol sequence $\{\beta_{1k}\}$ and have averaged over ϕ . Note that the worst case curves are about 2 dB worse than the average results. Also, note that the worst case results in Table III are slightly greater because they include the worst value of ϕ .

Fig. 12 shows the coded 16-QAM, memory $\nu = 2$ coding case with an interference compensator. The average error event probability is calculated by the method of moments for the parallel transition minimum distance error event and the

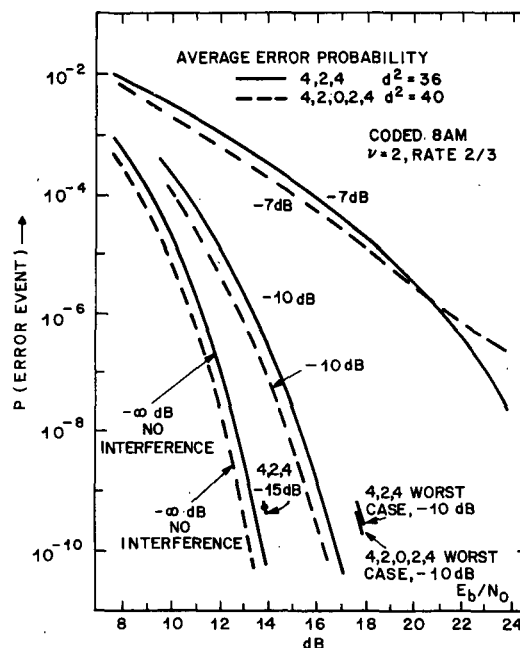


Fig. 11. Average error event probability for rate $2/3$, $\nu = 2$ coded 8-AM with interference compensation. For comparison we have also shown some worst case values.

next minimum distance error event. Some error event probabilities based on the worst transmitted sequence (denoted S_{1R} , S_{1I} worst case on the figure) are also shown for comparison. After comparison to the uncoded 16-QAM in Fig. 9 and 8-AMPM in Fig. 10 and to Table II, we can conclude that this code has some interference suppression capability, i.e., the coding gain without interference is smaller than the coding gain with limited interference, for instance, for ξ at -10 dB and an error event probability of 10^{-8} , an additional 2 dB coding gain is achieved relative to the case where $\xi_1 = 0$. This is also the case for the same coded 16-QAM scheme with no interference compensation, as was discussed earlier (see Figs. 5, 7, and 8)

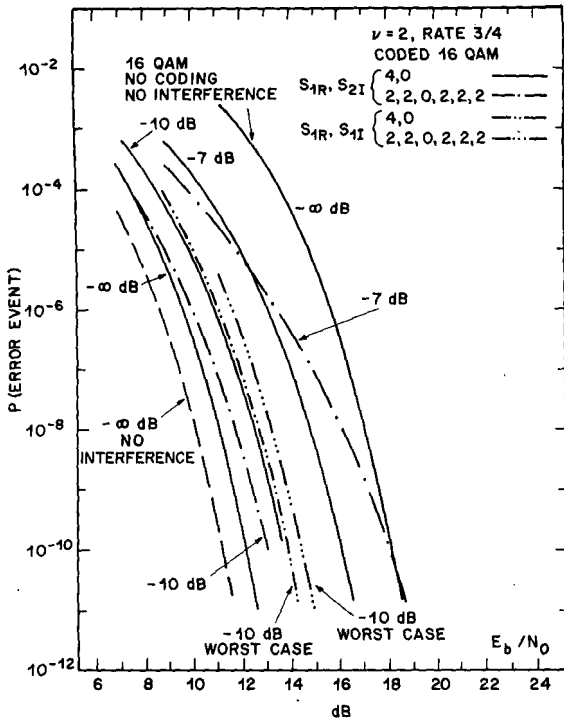


Fig. 12. Average and worst case error event probabilities for rate 3/4, $\nu = 2$ coded 16-QAM. Interference compensation is used. The S_{1R} , S_{2I} cases are calculated for $\xi_1 = \xi_2$.

Finally, we show some error event probability results for the coded 16-QAM case with the diagonal $\Delta s = \{4, 4\}$ parallel transition, that is, for example, signal point $(0, 0, 0, 0)$ versus $(1, 1, 0, 0)$ in Fig. 3. The results referred to as worst case error event probability in Fig. 13 are average error probability for the worst transmitted sequence. These results display similar relative behavior to the $\Delta s = \{4, 0\}$ parallel transition shown in Fig. 12. This is also consistent with Table II. The coding gains are, of course, larger for the scheme in Fig. 13. Longer error events must, however, also be considered before any conclusions can be made as to how well this code performs with interference.

VI. SUMMARY AND CONCLUSIONS

Bandwidth efficient, combined quadrature amplitude modulation (QAM) and simple convolutional codes (Ungerboeck-type) have been considered when, in multidimensional transmission, cross-coupling interference is present. This type of coding can be applied either on one of two rails of each QAM signal, or jointly on the two rails. Using these methods, coding gains can be obtained without any bandwidth expansion. In the paper we have analyzed average error event probabilities for some bandwidth efficient combined coding and modulation methods for a class of cross-coupled interference channels, both with and without interference compensation. Our conclusions are as follows.

- 1) Through extensive numerical computations, our results indicate that with cross-coupling interference, the coding gains from the interference free channels are preserved or even extended. This is true both with and without interference compensation.
- 2) The coding gains are larger for the case of combined coding on the two rails. Also, we find that for independently cross-coupled channels, coding on two rails that belong to two different QAM signals can provide diversity gain in the form of total system throughput increase via prolonged availability of the two QAM signals.
- 3) The analysis tools used are the method of moments to

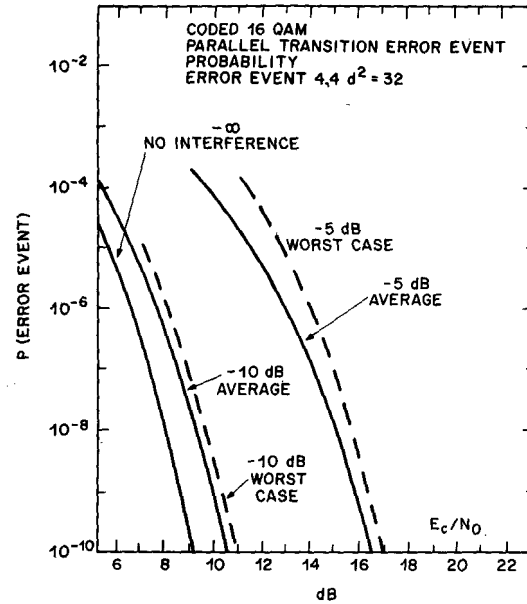


Fig. 13. Average and worst case event probabilities for the minimum distance parallel transition error event of the $\nu = 8$, rate 3/4 coded 16-QAM scheme. Interference compensation is used.

obtain quite exact average error event probabilities and simple worst case formulas for the error event probabilities. Thus, we can base our conclusions on precise lower bounds and on asymptotic coding gain in E_b/N_0 , which is based on worst case interference for dominating error events.

- 4) Our formulas are general and it is quite straightforward to extend the numerical results to larger constellations. For example, the relative performance of a rate 5/6 coded 64-QAM or 32-AMPM is very similar to rate 3/4 coded 16-QAM or 8-AMPM in terms of relative coding gains and interference suppression. The same holds for one-rail coding.

In summary, our paper demonstrates that trellis codes can yield significant error performance gains for multidimensional QAM systems in the presence of cross-coupling between signal dimensions. In later work, error event analysis has been extended to bit error probability evaluation for a larger family of codes, and the results further confirm the good behavior of the trellis codes considered herein. Future work should consider models for dispersive fading and codes that are compatible with carrier and timing recovery techniques for receiver implementation.

APPENDIX

This Appendix presents a description of the moments required to evaluate the error probabilities in the paper.

A. Moments for (14)

The moments for $Y' = Y/C$ with Y given in (14) can be computed from

$$E \{ Y'^{2J} \} = \xi_1^{2J} E \{ [\delta_{2k} \cos \phi_1 - \beta_{2k} \sin \phi_1]^{2J} \} \quad (A-1)$$

where, as the interference probability density function has even symmetry, all the odd moments are zero. Now, because

$$\frac{1}{2\pi} \int_0^{2\pi} (a \sin x + b \cos x)^{2n} dx = \frac{(2n-1)!!}{(2n)!!} \cdot (a^2 + b^2)^n \quad (A-2)$$

where

$$(2n)!! = 2 \cdot 4 \cdots (2n) = 2^n \cdot n! \quad (A-3)$$

$$(2n-1)!! = 1 \cdot 3 \cdots (2n-1) = \frac{(2n-1)!}{2^{n-1}(n-1)!} \quad (\text{A-4})$$

and $n!$ represents n factorial, there follows

$$E\{Y^{2J}\} = \xi_1^{2J} \frac{(2J-1)!!}{(2J)!!} E\{(\delta_{2k}^2 + \beta_{2k}^2)^J\}. \quad (\text{A-5})$$

Using the independence of δ_{2k} and β_{2k} and the binomial rule, we can expand (A-5) as

$$E\{Y^{2J}\} = \xi_1^{2J} \frac{(2J-1)!!}{(2J)!!} \sum_{i=0}^J \binom{J}{i} E\{\delta_{2k}^{2i}\} E\{\beta_{2k}^{2(J-i)}\}. \quad (\text{A-6})$$

In (A-6) the averages can simply be carried out over the multilevel, uniformly distributed symbols δ_{2k} and β_{2k} .

B. Moments for (23)

The moments of $Z' = Z/C$ with Z given in (23) can easily be found from

$$E\{Z^{2J}\} = \xi_1^{2J} \xi_2^{2J} E\{(\cos \phi - \beta_{1k} \sin \phi)^{2J}\}. \quad (\text{A-7})$$

Use of the integral in (A-1) gives

$$E\{Z^{2J}\} = (\xi_1 \xi_2)^{2J} \frac{(2J-1)!!}{(2J)!!} E\{(1 + \beta_{1k}^2)^J\} \quad (\text{A-8})$$

and this is simply solved as described for the similar case in Section A.

C. Moments for (39) and (40)

The moments required are those of X in (39), which depend on the independent random variables ϕ , β_{1k} , and δ_{1k} , $k = 1, 2, \dots$. Now we can express the sum in (39) as a sum of weighted independent random variables, that is, $\Delta = \sum_k u_k \cdot \theta_k$ where u_k 's are the weights and θ_k 's are the random variables. For $\xi_1 = \xi_2 = \xi$

$$E\{X^{2J}\} = \xi^{4J} E\left\{\left[\cos \phi - \frac{2}{d_{ij}^2} \sin \phi (\sum_k u_k \theta_k)\right]^{2J}\right\}. \quad (\text{A-9})$$

Averaging first with respect to ϕ and using Sections A and B, there follows

$$E\{X^{2J}\} = \xi^{4J} \frac{(2J-1)!!}{(2J)!!} E\left\{\left[1 + \left(\frac{2\Delta}{d_{ij}^2}\right)^2\right]^J\right\}. \quad (\text{A-10})$$

Again using the binomial theorem in (A-10), the moments can be found. To compute the moments of Δ in (A-10), we used the independence of the θ_k 's and Prabhu's algorithm, described in [17].

REFERENCES

- [1] A. Gersho and V. B. Lawrence, "Multidimensional signal constellations for voiceband data transmission," *IEEE J. Select. Areas Commun.*, vol. SAC-2, pp. 687-703, Sept. 1984.
- [2] M. Kavehrad, "Performance of cross-polarized M -ary QAM signals over nondispersive fading channels," *AT&T Bell Lab. Tech. J.*, vol. 63, pp. 499-521, Mar. 1984.
- [3] G. Ungerboeck, "Channel coding with multilevel/phase signals," *IEEE Trans. Inform. Theory*, vol. IT-28, pp. 55-67, Jan. 1982.
- [4] H. K. Tharpar, "Real-time application of trellis coding to high-speed voiceband data transmission," *IEEE J. Select. Areas Commun.*, vol. SAC-2, pp. 648-659, Sept. 1984.
- [5] L.-F. Wei, "Rotationally invariant convolutional channel coding with expanded signal space, Part I and Part II," *IEEE J. Select. Areas Commun.*, vol. SAC-2, pp. 659-686, Sept. 1984.
- [6] A. R. Calderbank and N. J. A. Sloane, "Four-dimensional modulation with an eight-state trellis code," *AT&T Tech. J.*, vol. 64, pp. 1005-1018, May-June 1985.
- [7] S. G. Wilson *et al.*, "Four-dimensional modulation and coding: An alternative to frequency reuse," in *Proc. Int. Conf. Commun.*, 1984, pp. 919-923.
- [8] G. H. Golub and J. H. Welsh, "Calculations of Gauss quadrature rules," *Math. Comput. J.*, vol. 26, pp. 221-230, Apr. 1969.
- [9] M. Kavehrad, "Performance of nondiversity receivers for spread spectrum in indoor wireless communications," *AT&T Tech. J.*, vol. 64, July-Aug. 1985.
- [10] P. J. McLane, "A residual intersymbol interference error bound for truncated-state Viterbi detectors," *IEEE Trans. Inform. Theory*, vol. IT-26, pp. 548-553, Sept. 1980.
- [11] W. U. Lee and F. S. Hill, Jr., "A maximum-likelihood sequence estimator with decision-feedback equalization," *IEEE Trans. Commun.*, vol. COM-25, pp. 971-979, Sept. 1977.
- [12] G. C. Clark and J. B. Cain, *Error-Correction Coding for Digital Communications*. New York: Plenum, June 1981.
- [13] S. Benedetto, M. Ajmone Marsan, G. Albertengo, and E. Giachin, "Combined coding and modulation: Theory and applications," Politecnico di Torino, Torino, Italy, Tech. Rep., Jan. 1985.
- [14] G. D. Forney, R. G. Gallager, G. R. Lang, F. M. Longstaff, and S. U. Qureshi, "Efficient modulation for band-limited channels," *IEEE J. Select. Areas Commun.*, vol. SAC-2, pp. 632-647, Sept. 1984.
- [15] S. G. Wilson and H. Y. Chung, "Multi-mode modulation and coding of QAM," Univ. Virginia, Charlottesville, Tech. Rep. UVA/528219/EE85/104, Aug. 1984.
- [16] N. K. Srinath, "Trellis codes in four dimensions: Design and performance evaluation," M.S.E.E. thesis, Univ. Virginia, Charlottesville, Aug. 1984.
- [17] V. K. Prabhu, "Some considerations of error bounds in digital systems," *Bell Syst. Tech. J.*, vol. 50, pp. 3127-3152, Dec. 1971.

★

Mohsen Kavehrad (M'78-SM'86), for a photograph and biography, see this issue, p. 1189.

★



Peter J. McLane (S'68-M'69-SM'80) was born in Vancouver, B.C., Canada, on July 6, 1941. He received the B.A.Sc. degree from the University of British Columbia, Vancouver, in 1965, the M.S.E.E. degree from the University of Pennsylvania, Philadelphia, in 1966, and the Ph.D. degree from the University of Toronto, Toronto, Ont., Canada, in 1969. He held a Ford Foundation Fellowship at the University of Pennsylvania and a National Research Council of Canada Scholarship at the University of Toronto.

From 1966 to 1967 he was a Junior Research Officer with the National Research Council, Ottawa, Ont. He held summer positions there in 1965 and 1966 and with the Defence Research Board of Canada in 1964. He joined the Department of Electrical Engineering, Queen's University, Kingston, Ont., in 1969 as an Assistant Professor, and since 1978 he has held the rank of Professor. His research interests are in signal processing for digital communication systems and radar. Usually this involves computer-aided analysis, but of late he has been involved in experimental work involving microprocessors and LSI-based implementation. He has served as a consultant to the Canadian Department of Communication and the Canadian Institute of Guided Ground Transport. During 1984-1985 he was on leave at AT&T Bell Laboratories Crawford Hill Laboratory, Holmdel, NJ.

Dr. McLane has been active in the IEEE Communications Society. He is a member of the Communication Theory Committee and served as representative on the Technical Program Committee of the 1978 International Conference on Communications. At present he is an Associate Editor for the IEEE COMMUNICATIONS MAGAZINE and the IEEE TRANSACTIONS ON

COMMUNICATIONS. He is also a member of the Association of Professional Engineers of Ontario and Eta Kappa Nu, and is listed in *American Men and Women of Science*.



Carl-Erik W. Sundberg (S'69-M'75-SM'81) was born in Karlskrona, Sweden, on July 7, 1943. He received the M.S.E.E. and Dr. Techn. degrees from the Lund Institute of Technology, University of Lund, Lund, Sweden, in 1966 and 1975, respectively.

Currently he is a member of the Technical Staff at AT&T Bell Laboratories, Holmdel, NJ. Before 1976 he held various teaching and research positions at the University of Lund. During 1976, he was with the European Space Research and Technology Centre (ESTEC), Noordwijk, The Netherlands, as an ESA Research Fellow. From 1977 to 1984 he was a Research Professor (Docent) in the

Department of Telecommunication Theory, University of Lund. He has held positions as Consulting Scientist at LM Ericsson, SAAB-SCANIA, Sweden, and at Bell Laboratories, Holmdel. His consulting company, SUNCOM, has been involved in studies of error control methods and modulation techniques for the Swedish Defense, a number of private companies, and international organizations. His research interests include source coding methods, channel coding (especially decoding techniques), digital modulation methods, fault-tolerant systems, digital mobile radio systems, spread-spectrum systems, and digital satellite communications systems. He has published over 40 journal papers and contributed over 50 conference papers. He holds several Swedish and international patents.

Dr. Sundberg has been a member of the IEEE European-African-Middle East Committee (EAMEC) of COMSOC from 1977 to 1984. He has also been a member of the Technical Program Committees for the International Symposium on Information Theory, St. Jovite, Canada, October 1983, and for the International Conference on Communications, Amsterdam, The Netherlands, May 1984. He has organized and chaired sessions at a number of international meetings. He is a member of SER (Svenska Elektroingenjörers Riksförening) and the Swedish URSI Committee (Svenska Nationalkommittén för Radiovetenskap).